

AUS Repository

Kinetics of Ultrasonic Drug Delivery from Targeted Micelles

Item Type	Peer-Reviewed;Article;Published version
Authors	Husseini, Ghaleb;Kherbeck, Laura;Pitt, William G.;Christensen, Douglas A.;Velluto, Diana
Citation	Husseini, G. A., Kherbeck, L., Pitt, W. G., Hubbell, J. A., Christensen, D. A., & Velluto, D. (2015). Kinetics of ultrasonic drug delivery from targeted micelles. <i>Journal of Nanoscience and Nanotechnology</i> , 15(3), 2099–2104. https://doi.org/10.1166/jnn.2015.9498
DOI	10.1166/jnn.2015.9498
Publisher	American Scientific Publishers
Download date	2026-06-08 03:07:23
Link to Item	http://hdl.handle.net/11073/19740

Kinetics of Ultrasonic Drug Delivery from Targeted Micelles

Ghaleb A. Hussein^{1,*}, Laura Kherbeck¹, William G. Pitt², Jeffrey A. Hubbell³,
Douglas A. Christensen⁴, and Diana Velluto³

¹Chemical Engineering Department, American University of Sharjah, United Arab Emirates

²Bioengineering Department, Ecole Polytechnique Federale de Lausanne, Switzerland

³Chemical Engineering Department, Brigham Young University, Provo, 84602, Utah

⁴Department of Bioengineering, University of Utah, SLC, 84112, Utah

To minimize the adverse side effects of conventional chemotherapy, a targeted micellar drug carrier was investigated that retains hydrophobic drugs in its core and then releases the drug via ultrasonic activation. This paper compares the percent drug release from folated versus non-folated micelles by insonation at 70 kHz and different acoustic power densities. The encapsulated drug is Doxorubicin (Dox). A physical model of zero-order release with first-order re-encapsulation was used to fit the experimental kinetic data. Additionally, the acoustic activation power density and Gibbs free energy were introduced and calculated for folated and non-targeted micelles. The data suggests an important role of inertial cavitation in drug release and the presence of a power density threshold for inertial cavitation. IP: 129.7.158.43 On: Thu, 08 Jan 2015 14:18:35

Keywords: Folated Micelles, Kinetic Models, 70-kHz Ultrasound, Pluronic P105, Drug Release, Re-encapsulation, Targeted Drug Delivery.

1. INTRODUCTION

Conventional chemotherapy has always been accompanied by debilitating side-effects; therefore the ability to sequester chemotherapy drugs inside a nanocarrier that would release them only when and where needed is a significant advancement.¹ The main premise of this work is that the drug is released from the nanocarrier upon the application of an external stimulus, namely ultrasound. Ultrasound can be considered an ideal trigger since it is non-invasive and painless.² Moreover, ultrasonic waves propagate deep into the body and can be accurately focused on the tumor site. It also has a synergistic effect on drug activity brought about by what is believed to be enhanced drug transport across the cell membrane of tumor cells.³ Low ultrasound frequencies, in the range of 20 kHz to 100 kHz, cause the highest drug release from micelles.⁴ Current theory claims that acoustically-activated micellar drug delivery systems are rendered effective due to two main mechanisms. First, ultrasound results in drug release via bubble cavitation that disrupts the core of polymeric micelles. Second, ultrasonic

cavitation has been shown to form micropores in the membranes of cancer cells—a phenomenon called sonoporation—which allows drugs to passively diffuse into the cells.⁵

The proposed drug-delivery scenario is as follows. A hydrophobic drug is loaded into a nanocarrier, or a micelle, by the simple act of mixing. The micelles containing the sequestered drug are then administered to the patient via an IV injection and circulate throughout the body. Some extravasation into tumors occurs.⁶ In time, low-frequency ultrasound is applied to the tumor volume only, thereby stimulating the micelles to release their therapeutic content. Ultrasound both releases the drug from micelles and promotes intracellular uptake of both released and encapsulated drug.³ When the ultrasound is turned off, any remaining drug is re-encapsulated back into the carrier or is transported into nearby cells.

Given these advantages, micelles are not without disadvantages. They are prone to a short blood half-life due to at least 2 mechanisms. First, blood proteins are adsorbed onto the surface of these nanocarriers which makes them susceptible to recognition by the macrophages of the mononuclear phagocyte system (MPS).⁷ To enhance the carriers' circulation time in the blood, the carrier surface is

* Author to whom correspondence should be addressed.

modified via the addition of polyethylene glycol (PEG).⁸ Second, the micelles themselves can dissolve when diluted in blood below their critical micelle concentration.

The next step to improve the specificity of the carrier towards the cancer tissue, was to attach certain surface ligands that would bind the nanocarriers to the cell and in some cases stimulate endocytosis into the tumor cell. The way to render the nanocarrier more “appealing” to the tumor cell is achieved by conjugating ligands to the surface of the micelle. These targeted micelles can then bind to receptors on the surface of cancerous cells. Various tumors have been found to overexpress folate receptors. Thus, attachment of folate to the carrier surface was pursued by many labs.^{7–9}

Once these targeted carriers are synthesized, it is essential to measure the amount of drug released from their core as compared to non-targeted micelles and to study and eventually model the kinetic mechanisms by which the drug is released and subsequently re-encapsulated. To do so, mathematical models were developed to describe release and re-encapsulation kinetics.^{10–12}

The present study measures the release of Doxorubicin (Dox) from folated versus non-folated micelles at different acoustic power densities. Then, a zero-order release with first-order re-encapsulation physical model was used to mathematically model the kinetics of this drug delivery system in an attempt to better understand the physical mechanisms involved.

2. MATERIALS AND METHODS

2.1. Synthesis of Folated Pluronic Micelles

Pluronic P105 (BASF) with folate attached to its surface was conjugated using 1,1-carbonyldiimidazole (CDI, Sigma Aldrich).¹³ Folic acid (FA, Sigma Aldrich) was dissolved in dried DMSO. CDI was added and allowed to react for 4 hours under dark conditions at room temperature. After the activation of the FA, Pluronic P105 (dried overnight under vacuum) was added. The activated CDI and Pluronic P105 were reacted for 20 hours at room temperature in darkness. Next, the product was dialyzed (Spectra Millipore MWCO 3500) against DMSO for 2 days and then against double distilled water (DD-water) for 2 days. The purified product was then lyophilized and stored at -20°C . The formation of P105-FA was confirmed using NMR (48% yield). For release experiments, P105-FA was dissolved in DD-water to make a final concentration of 5 wt.%. Dox ($4.5\ \mu\text{g}/\text{ml}$) (Sigma Aldrich) was introduced into the micelles by mixing at room temperature. Using dynamic light scattering, the size of these micelles was measured to be $10.2 \pm 2.2\ \text{nm}$.

2.2. Ultrasonic Exposure Fluorescence Detection Chamber

To quantify the release, a custom chamber was built to measure the change in fluorescence and hence the Dox

release in the presence and absence of ultrasound.¹⁴ The beam of an argon ion laser (Ion Laser Technology, Model 5500 A) was directed to a beam splitter attenuator (metal film neutral density attenuator). The intensity of the split portion of the beam was measured by a photodetector (used to monitor the laser power) and the other portion of the beam was directed into a fiber optic bundle.

The drug concentration was quantified by measuring fluorescence emissions at 535 nm produced by an excitation wavelength of 488 nm. A fiber optic probe (100 bundled multimode fibers, approximately 40 cm in length) was used to deliver the excitation light to the sample and to collect fluorescence emissions. The emitted light was directed through a dielectric bandpass filter (Omega Optical Model 535DF35) to a silicon detector (EG & G 450-1). The filter was used to cut off any emissions below 517 nm, including any Rayleigh-scattered laser light. Fluorescence measurements were digitized for computer storage and processing. To mimic physiological conditions, the temperature of the ultrasonic exposure chamber was maintained at 37°C using a thermostated bath.

The chamber described above was used to measure the kinetics of acoustically activated drug release from the P105-FA micelles. Doxorubicin exhibits a large decrease in fluorescence when transferred from the hydrophobic core of the micelle to the surrounding aqueous solution. Therefore, the release can be determined by measuring the decrease in fluorescence intensity upon the application of ultrasound. In these release experiments, a Dox concentration of $4.5\ \mu\text{g}/\text{ml}$ was used. When calculating the percent release, fluorescence data were corrected to account for Dox quenching by folic acid. Ultrasound was applied using a 70-kHz ultrasonicating bath (SC-40, Sonicator, Copiaque, NY) equipped with a single piezoceramic transducer that is driven at approximately 70 kHz. The waveform can be described as a 70-kHz wave that is amplitude-modulated sinusoidally at about 0.12 kHz. The bath was powered by 60-Hz AC voltage from a variable AC transformer (variac). The voltage from the variac to the sonicating bath was adjusted to produce differing intensities of continuous ultrasound as measured using a hydrophone (Bruel and Kjaer model 8103, Decatur, GA). The ultrasound was manually turned on and off every 10 seconds.

The decrease in fluorescence of the encapsulated drug solution was assumed to be directly proportional to the amount of drug released relative to a known baseline. The fluorescence of Dox in PBS, in the absence of Pluronic, was measured to simulate 100% release. Then the percent release was calculated as follows:

$$\% \text{ release} = \frac{I_{P105} - I_{US}}{I_{P105} - I_{PBS}} \times 100\% \quad (1)$$

where, I_{US} is the fluorescence intensity upon exposure to ultrasound, I_{PBS} is the fluorescence intensity in a solution of Dox in PBS, and I_{P105} is the intensity recorded when the drug is encapsulated in Pluronic P105 (which corresponds to 0% release or 100% encapsulation).

3. DATA ANALYSIS

3.1. Comparison of Release from Folated and Non-Folated Micelles

The amount of Dox release as a function of ultrasound intensity was measured at a frequency of 70 kHz. We have previously reported the percent release of folated P105 micelles with ultrasonic power density.¹⁵ Here we compare the acoustic release from these targeted micelles to non-targeted Pluronic P105 micelles, and then apply a mathematical analysis to the data.

Figure 1 summarizes the percent of drug release from folate-targeted and non-targeted micelles as a function of acoustic power density. At low power densities, the measured drug release is very small and cannot be distinguished from noise in the control experiment where ultrasound was not applied. This trend continues up until about 0.5 W/cm², after which the release from folated micelles follows an almost linear increase with the power densities up until approximately 3 W/cm², which constitutes the second region on the plot. Meanwhile, the release from non-targeted micelles exhibits less linear behavior in this power density region. However, when greater than 1.03 W/cm² was applied, the release from non-targeted micelles is always lower than the release from the folated micelles. In the third region, above 3 W/cm², both types of micelles demonstrate a fairly constant amount of release, independent of acoustic power density. For folated micelles, this amounts to approximately 13%, while for the non-targeted micelles it is only about 10%.

The data show the existence of two thresholds, 0.5 W/cm² and 3 W/cm², which suggest the role of inertial cavitation in the drug release. The lower threshold value is believed to correspond with the onset of inertial cavitation in water. While there is yet no explanation for the upper threshold, it has been reported in other studies.¹⁶ At the lower threshold, a possible explanation is that onset of inertial cavitation produces shock waves that rupture the micelles, resulting in the release of the encapsulated drug into the aqueous environment. It can be

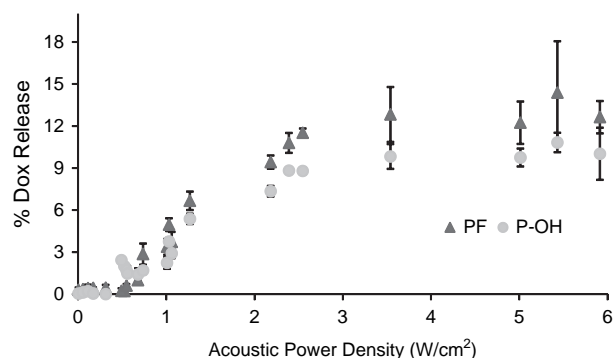


Figure 1. Percent release of Dox from targeted (triangles) and non-targeted (circles) micelles as a function of acoustic power density at 70 kHz.

hypothesized that the higher release from folated micelles can be attributed to the compromised structural integrity of the micelle structure due to the attached folic acid; i.e., the attached moiety has made the micelles less mechanically stable when subjected to shock waves and shear stresses from transient cavitation produced by low-frequency ultrasound.

3.2. Testing Statistical Significance

The non-parametric Mann–Whitney U test was conducted on the folated and non-targeted micellar acoustic release data for each power density in order to assess the statistical significance of experimental data. The Mann–Whitney test was chosen because the data were from two unpaired groups and did not follow a Gaussian distribution. The lower power densities did not have enough data points to give accurate results, but power densities of 1.03 W/cm² and higher all gave statistically significant levels ($\alpha = 0.05$ or less). Therefore, drug release from folated micelles is statistically significantly higher than release from non-targeted carriers.

4. MODELING THE RELEASE KINETICS

4.1. Model: Zero-Order Release and First-Order Re-Encapsulation

In previous studies, mechanistic and deterministic models were used to model ultrasonically activated drug delivery from polymeric micelles.^{10–12, 16–21} In this study, we used the model previously formulated by Husseini et al.¹⁰ The model proposes that Dox is released from micelles at a constant rate while the ultrasound is on, and the simultaneous rate of re-encapsulation is first-order with respect to the concentration of the free drug. This model is based on the theory that ultrasound may create inertial cavitation events that result in the destruction of micelles at a constant rate, and that this rate does not depend on the micelle concentration. The destroyed micelles release the drug, but the free Dox molecules are taken up by micelles at a rate proportional to the free drug concentration. The drug can either be re-encapsulated into micelles that were not destroyed, or into newly-formed micelles.⁶

Mathematically, the model can be represented using the equation:

$$\left. \frac{dE}{dt} \right|_{US} = -k_r + k_e F = -k_r + k_e (T - E) \quad (2)$$

where, E is the amount of drug encapsulated, F is the amount of free drug, T is total amount of the drug in solution, k_r is the zero-order release rate constant, and k_e is the first order re-encapsulation rate constant.

Rearranging and applying the integrating factor method gives

$$e^{k_e t} \frac{dE}{dt} + k_e e^{k_e t} E = (k_e T - k_r) e^{k_e t} \quad (3)$$

The left hand side of Eq. (5) follows the product rule, so the equation can be rewritten as:

$$\frac{d}{dt}(Ee^{k_e t}) = (k_e T - k_r)e^{k_e t} \quad (4)$$

Rearranging and dividing by $e^{k_e t}$ gives the amount of Dox encapsulated as a function of time during insonation:

$$E(t)|_{US} = \frac{k_r}{k_e} e^{-k_e t} - \frac{k_r}{k_e} + T \quad (5)$$

At long insonation times, E/T approaches the steady state drug concentration during US exposure, which is:

$$E/T|_{SS} = -\frac{k_r}{k_e T} + 1 \quad (6)$$

4.2. Data Fitting

The raw fluorescence data were noisy, and since the pulsing of the ultrasound was done manually, the exact on/off times do not coincide for all experiments. For each power density, several experimental runs were conducted, and then the regions were divided according to where release and re-encapsulation occurred. The curves of release versus time were plotted and were subsequently overlapped over the horizontal and vertical axes. The release and re-encapsulation regions were overlapped independently. Sample plots showing overlapped runs for release and re-encapsulation for folated micelles at the highest power

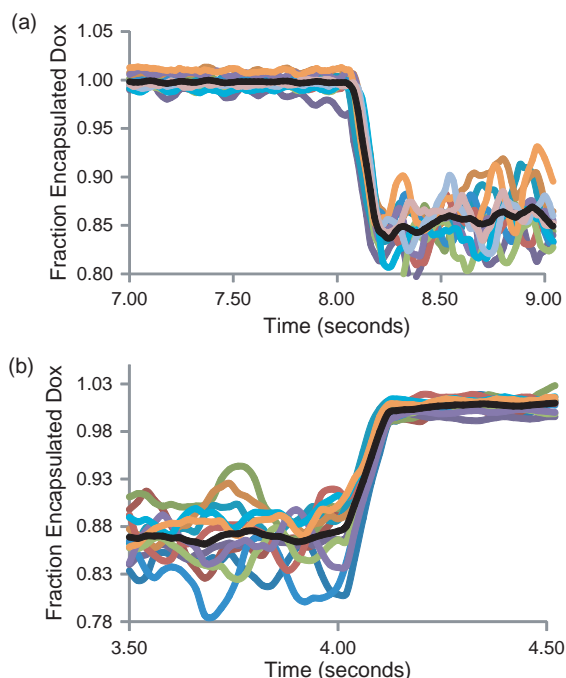


Figure 2. An example showing 12 overlaid ultrasound exposure cycles to determine the release and re-encapsulation averages when (a) the ultrasound was turned on and release started, and (b) when ultrasound was turned off and re-encapsulation began. Data shown are for folated micelles at 5.91 W/cm².

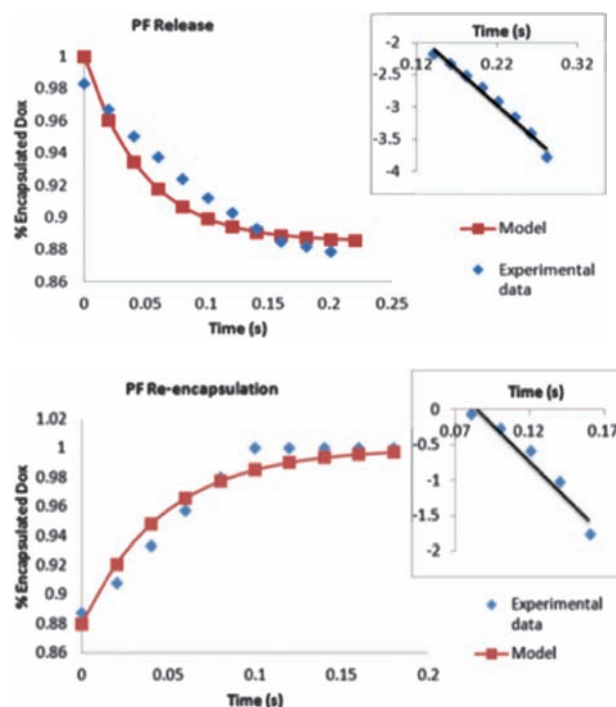


Figure 3. Typical release and re-encapsulation data from the experiment with folated micelles at 2.55 W/cm². The solid line is the model fit. The inserts are log transforms of the data and the model fit.

density are shown in Figure 2. The black line is the average of all 12 runs at 5.9 W/cm².

In Eq. (6), T is defined as the total amount of Dox in the solution and it is equal to 4.5 $\mu\text{g/ml}$. A plot of $\ln[(E/T - 1)/(E(t_{\text{off}})/T - 1)]$ versus time, gave a slope equal to the value of the re-encapsulation rate constant, k_e . $E(t_{\text{off}})/T$ was obtained from the plot.

As seen in the mathematical model, the release constant, k_r , was then obtained as such:

$$k_r = Rk_e T \quad (11)$$

where R , the fraction of drug released, corresponds to $(1 - E/T)$.

The data in Figure 3 were then generated for all power densities for release and re-encapsulation to test how well the mathematical model fit the data. The inserts show the log transforms of the data and the model fit which were initially used to test the model.

4.3. Acoustic Activation Power Density and Gibbs Free Energy

Figure 4 depicts the physical meaning of activation power density. To obtain the acoustic activation power density, a model analogous to a process with an activation energy is employed:

$$k_r = A e^{-PD_a/PD} \quad (12)$$

Where, k_r is the zero-order release rate constant, A is the pre-exponential factor, PD is the power density and PD_a is the acoustic activation power density.

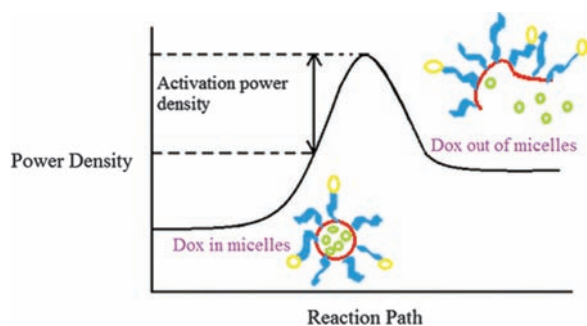


Figure 4. Plot showing the activation power density necessary to release encapsulated Dox from micelles.

Thus, a plot of $\ln(k_r)$ versus $1/PD$, would yield a slope that corresponds to $-PD_a$, or the negative of the acoustic activation power density, and the logarithm of the analogous Arrhenius pre-exponential factor from the intercept. The plot is shown in Figure 5.

The Gibbs free energy is given by

$$\Delta G = -RT \ln K_{eq} = -RT \ln \frac{k_r}{k_e} \quad (13)$$

Thus for folated micelles, $k_r = 15.30e^{-1.30/PD}$. Since k_e is almost constant, it is averaged over all power densities (\bar{k}_e). Thus, the Gibbs free energy for each power

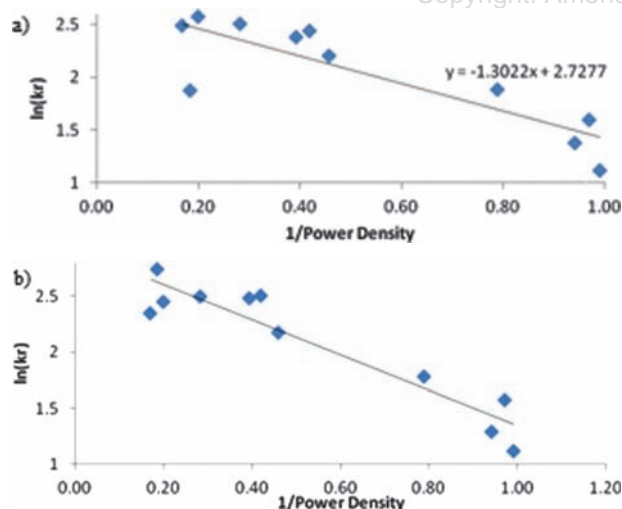


Figure 5. Plots used to find the acoustic activation power density for release for (a) folated micelles and (b) non-folated micelles.

Table I. Summary of Acoustic Activation Power Density and Pre-exponential Factor.

	Acoustic activation power density (W/cm ²)	Pre-exponential factor (μg/ml·s)
PF	1.30	15.30
P105	1.57	18.47

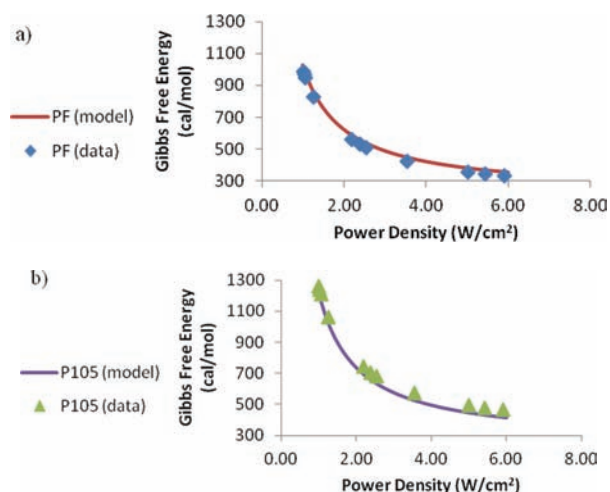


Figure 6. A plot showing the Gibbs free energy as a function of power density for (a) folated micelles and (b) non-folated micelles.

density is calculated using Eq. (14):

$$\Delta G = -RT \ln \left[\frac{15.30e^{-(1.30/PD)}}{\bar{k}_e} \right] \quad (14)$$

The Gibbs free energy obtained from the model for both folated and non-folated micelles is plotted and compared to the values given by the data. The results are shown in Figure 6 and the model agrees with the data well.

5. CONCLUSION

The percent acoustic drug release from folate-targeted Pluronic P105 micelles loaded with Doxorubicin (Dox) has been investigated and the results were compared to the release from non-targeted micelles under the same conditions of low-intensity ultrasound at different acoustic power densities. It was found that folated micelles exhibit greater drug release than non-folated micelles. Furthermore, the presence of a power density threshold indicates that inertial cavitation plays a role in acoustic drug release from micelles. Release and re-encapsulation data were fitted using a zero-order release/first-order re-encapsulation model. Finally, we also introduced the concept of an acoustic activation power density which is analogous to the activation energy in an activated process. The activation power density indicates that there is an energy barrier to overcome in order to observe measurable release.

References and Notes

- G. A. Husseini, G. D. Myrup, W. G. Pitt, D. A. Christensen, and N. Y. Rapoport, *J. Controlled Release* 69, 43 (2000).
- H. Zhang, H. Xia, J. Wang, and Y. Li, *J. Controlled Release* 139, 31 (2009).
- D. Chen and J. Wu, *Ultrasonics* 50, 744 (2010).
- G. Myhr and J. Moan, *Cancer Lett.* 232, 206 (2006).
- G. A. Husseini and W. G. Pitt, *J. Pharm. Sci.* 98, 795 (2009).
- B. J. Staples, B. L. Roeder, G. A. Husseini, and W. G. Pitt, *J. Pharm. Sci.* 99, 3122 (2010).

7. B. Stella, S. Arpicco, M. T. Peracchia, D. Desmaële, J. Hoebeke, M. Renoir, J. D'Angelo, L. Cattel, and P. Couvreur, *J. Pharma. Sci.* 89, 1452 (2000).
8. A. Gabizon, H. Shmeeda, A. T. Horowitz, and S. Zalipsky, *Adv. Drug Deliv. Rev.* 56, 1177 (2004).
9. R. J. Lee and P. S. Low, *Biochimica et Biophysica Acta* 1233, 134 (1995).
10. G. A. Husseini, N. Y. Rapoport, D. A. Christensen, J. D. Pruitt, and W. G. Pitt, *Coll. Surf. B: Biointerfaces* 24, 253 (2002).
11. D. Stevenson-Abouelnasr, G. A. Husseini, and W. G. Pitt, *Coll. Surf. B: Biointerfaces* 55, 59 (2007).
12. G. A. Husseini, M. A. De la Rosa, E. O. AlAqqad, S. Al Mamary, Y. Kadimati, A. Al Baik, and W. G. Pitt, *J. Franklin Institute* 348, 125 (2011).
13. S. Huang, S. Sun, T. Feng, K. Sung, W. Lui, and L. Wang, *European J. Pharm. Sci.* 38, 64 (2009).
14. G. A. Husseini, G. D. Myrup, W. G. Pitt, D. A. Christensen, and N. Y. Rapoport, *J. Controlled Release* 69, 43 (2000).
15. G. A. Husseini, D. Velluto, L. Kherbeck, W. G. Pitt, J. A. Hubbell, and D. A. Christensen, *Coll. Surf. B: Biointerfaces* 101, 153 (2012).
16. G. A. Husseini, M. A. Diaz, Y. Zeng, D. A. Christensen, and W. G. Pitt, *J. Nanosci. Nanotechnol.* 7, 1 (2007).
17. G. A. Husseini, N. M. Abdel-Jabbar, F. S. Mjalli, and W. G. Pitt, *Technol. Cancer Res. Treat.* 6, 49 (2007).
18. G. A. Husseini, F. S. Mjalli, W. G. Pitt, and N. M. Abdel-Jabbar, *Technol. Cancer Res. Treat.* 8, 479 (2009).
19. M. A. Diaz de la Rosa, G. A. Husseini, and W. G. Pitt, *Ultrasonics* 53, 97 (2013).
20. M. A. Diaz de la Rosa, G. A. Husseini, and W. G. Pitt, *Ultrasonics* 53, 377 (2013).
21. G. A. Husseini, N. M. Abdel-Jabbar, F. S. Mjalli, W. G. Pitt, and A. Al-Mousa, *J. Franklin Institute* 348, 1276 (2011).

Received: 10 June 2013. Accepted: 29 December 2013.

Delivered by Publishing Technology to: University of Houston
IP: 129.7.158.43 On: Thu, 08 Jan 2015 14:18:35
Copyright: American Scientific Publishers